



ORIGINAL ARTICLE OPEN ACCESS

Evaluating the Efficacy of Low Salinity Waterflood and Electrokinetic Enhanced Oil Recovery in Mitigating Gas Condensate Banking

Princewill M. Ikpeka¹  | Chidiebele E. J. Uzoagba² 

¹Global Challenges and Transdisciplinary Change, Brunel University, Uxbridge, UK | ²Petroleum and Energy Resources Engineering Department, African University of Science and Technology (AUST) Abuja, Abuja, Nigeria

Correspondence: Princewill M. Ikpeka (Princewill.ikpeka@brunel.ac.uk)

Received: 8 May 2025 | **Revised:** 14 September 2025 | **Accepted:** 28 October 2025

Keywords: electrokinetic enhanced oil recovery | gas condensate | low-salinity water | sustainability

ABSTRACT

Condensate banking is a key challenge for gas condensate reservoirs with low permeability as it reduces gas relative permeability as much as ~60% near the wellbore. Condensate banking occurs when the bottom-hole pressure in the near-well bore region falls below the dew-point pressure of the gas. This study investigates condensate-banking treatment using a combined low-salinity waterflooding (LSW) and electrokinetic enhanced oil recovery (EK-EOR) techniques. The theoretical framework proposed in this paper is derived from the principles of fluid-rock interaction, electrokinetic phenomena, and water salinity. Methodologically, results from IFT laboratory experiments were fed into simulation models and used to evaluate the effectiveness of LSW-EKEOR treatment. Numerical simulations were performed using a synthetic reservoir model that captures typical reservoir conditions, including pressure, temperature, fluid properties, and rock characteristics. The results show that combining LSW with EKEOR increases condensate recovery by 228%, primarily by reducing gas condensate accumulation—particularly in high-permeability zones. Additionally, the approach suggests a potentially superior environmental performance by lowering the energy required for treatment and reducing chemical use. The discussion explores the broader implications of this technique for future oil recovery processes, emphasizing its potential to reduce operational costs and carbon footprints in mature fields.

1 | Introduction

The increasing demand for sustainable and cleaner energy, in addition to the need for reliable energy, has skewed interests to natural gas as a cleaner and more efficient energy source. Among all hydrocarbon energy sources, natural gas and condensate provide the lowest carbon footprint during its lifecycle use and is thought to be a viable long-term solution to meet the increasing energy needs of the world [1]. The environmental and price benefits associated with natural gas and condensates are perhaps the biggest reason for the preferential increase in natural gas consumption by all sectors (Figure 1).

Significant amounts of natural gas reservoirs exist as condensates; according to [2], 68% of all giant gas reservoirs discovered in the world exist as condensate reservoirs. One major problem cutting across these reservoirs is called condensate banking [3, 4]. It reduces the productivity of these reservoirs by as much as 60% in tight gas reservoirs, traps substantial amounts of valuable condensate and results in low return on investment [5]. Condensate banking occurs when the reservoir pressure declines below the dewpoint (saturation) pressure of the gas condensate [6, 7]. Previous studies have proposed several techniques to treat gas condensate banking such as; injection of solvents and alcohols (i.e., methanol) to reduce the interfacial

This is an open access article under the terms of the [Creative Commons Attribution](https://creativecommons.org/licenses/by/4.0/) License, which permits use, distribution and reproduction in any medium, provided the original work is properly cited.

© 2025 The Author(s). *Energy Science & Engineering* published by Society of Chemical Industry and John Wiley & Sons Ltd.

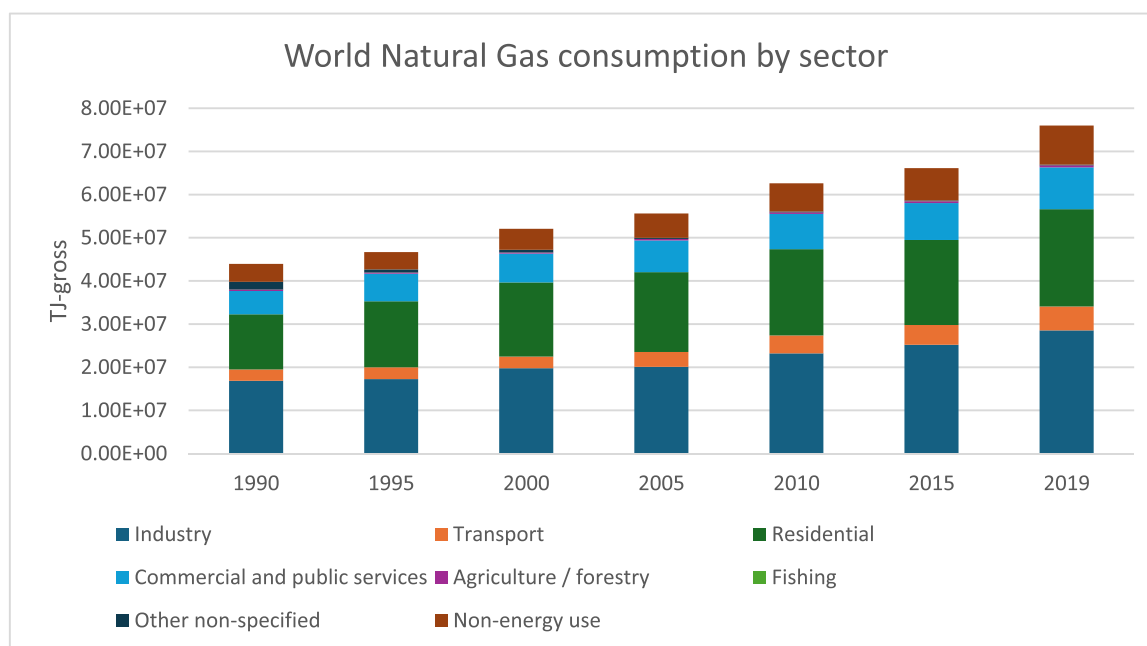


FIGURE 1 | Natural gas yearly consumption (source: <https://www.iea.org/data-and-statistics/data-product/natural-gas-information>).

tension (IFT) [3], injection of surfactants, polymers and nanoparticles to alter the wettability of the reservoir rock from water wet to preferentially gas [8, 9], injecting acids to improve permeability [10, 11], injecting gas or water-alternating-gas injection to maintain reservoir pressure above dew point pressure [12, 13], and introducing electric current to support the hydrodynamic condition of the reservoir to yield more condensate. The limitations of each of these techniques are highlighted by [4], these include; degradation of acids at high temperature, high cost of solvents/alcohols due to the need for regular injection, sensitivity of in-situ clay particles within the reservoir to solvents, potential severe pore throat blockage and irreversible well damage due to reservoir rock wettability alteration, etc. Consequently, there is an apparent need to explore relatively low-cost and environmentally beneficial methods of treating condensate banks.

The injection of low salinity brine as a treatment method for condensate-banking is relatively new [14]. Conventionally, waterflooding is used primarily as a pressure maintenance mechanism. However, when used to treat condensate-banking, low salinity waterflooding is used to drive the condensate from the near-wellbore regions into the production well. The ability to do this effectively depends on the IFT acting between the brine and the condensate molecules. A lower IFT increases the oil displacement efficiency of the brine [15]. This is largely due to the multicomponent ionic exchange between the rock mineral surface and the displacing low-salinity brine. The potential for treating condensate banks using low-salinity waterflooding (LSW) in sandstone reservoirs has high interest because of its relatively low cost and environmental benefits [16].

Another interesting method of treating condensate banks is the use of electric current to alter the IFT between the condensate and the water-wet rock surface in a process known as electrokinetic enhanced oil recovery (EK-EOR). The introduction of direct current into the pore space activates mechanisms which

enhance condensate flow. These include: movement of charged ions, drag force transfer of water molecules associated with charged ion movement, disintegration of water molecules into constituent gaseous and ionic phases, movement of colloid particles, viscosity reduction and thermal mobility of condensate fluid [17, 18]. Results from the IFT measurement obtained from experiments performed by [4], reveal a progressive increase in IFT as the voltage is increased.

Therefore, the objective of this study is to compare the effectiveness of LSW combined with EK-EOR method for the treatment of a condensate-bank. To do this, a compositional reservoir model was built using CMG-GEM, and the performance of both mechanisms (EK-EOR and LSW) were simulated by altering the IFT properties using data from both experiments and published sources. However, before describing the reservoir model, the theoretical framework for the effectiveness of both mechanisms needs to be outlined.

2 | Conceptual Framework

Relative permeability is important when two or more fluids flow simultaneously through a porous medium. For gas condensate reservoirs, depending on the prevailing reservoir pressure, 3 phases (condensate, gas, and water) could be anticipated to flow simultaneously. As the saturations of each flowing fluid changes, they interfere with the other flowing fluid. The relative permeability profile of a reservoir is the most effective way of predicting the effectiveness of a displacement mechanism. From the perspective of fluid flow mechanics, the residual condensate saturation is determined by two main forces: capillary and viscous forces. The microscopic displacement efficiency of any EOR method will depend on the relative influence of each of these two forces. The ratio of viscous forces to capillary forces is defined by [19, 20] as capillary number (Equation 1).

$$N_c = \frac{\mu_w}{\varphi} \frac{V_w}{\sigma_{wo}}, \quad (1)$$

where N_c , Capillary Number, μ_w , viscosity of the displacing phase, V_w , flow velocity of the displacing phase, φ , effective porosity of the formation and σ_{wo} is the water-oil IFT.

For EK-EOR treatment of condensate banked reservoirs, the reservoirs are flooded with low salinity brine in the presence of direct current. The microscopic efficiency of the displacement process is determined using Equation (2):

$$E_m = \frac{1 - S_{or} - S_{wc}}{1 - S_{wc}}, \quad (2)$$

where E_m , microscopic efficiency, S_{or} , residual oil saturation, and S_{wc} , residual water saturation.

Laboratory experiments conducted by [21–23], show a strong relationship between capillary number and residual oil saturation. Higher capillary number improves the microscopic displacement efficiency [20]. EK-EOR and LSW are both effective in increasing the capillary number, as they reduce the IFT between the displacing and displaced phase [24, 25].

The effect of EK-EOR for treating condensate banking is summarized by Equation (3), from laboratory experiment conducted by [4].

$$\text{Effect of Applied voltage} = \left\{ \begin{array}{l} \text{Change in} \\ \text{Permeability} \end{array} \right\} + \left\{ \begin{array}{l} \text{Change in} \\ \text{Interfacial Tension} \end{array} \right\}. \quad (3)$$

To simplify the analytical model for EK-EOR effect on relative permeability, the following assumptions were made:

1. The fluid flow is under steady state and its intrinsic properties are independent of local electric field, ion concentration, and temperature.
2. No slip-boundary conditions exist at the condensate-water interface

Based on a cylindrical core sample, the increment in oil flow-rate from EK-EOR process is captured by Equation (4).

$$q_t = \frac{A}{\mu} \cdot \frac{K \cdot \Delta p}{L} + \frac{A}{\mu} \cdot \frac{K_e \cdot E}{L}, \quad (4)$$

where K , Darcy permeability, K_e , electro-osmotic permeability, while μ is the viscosity and A & L represent cross-sectional area and length of core sample. Also, because the effect of electric current is applied to both the oil and water phase, the coupled flow under applied electric gradient can be represented using four relative permeability coefficients in Equation (5).

$$K_e = \begin{bmatrix} K_{e-oo} & K_{e-ow} \\ K_{e-wo} & K_{e-ww} \end{bmatrix}, \quad (5)$$

where the subscripts oo, ow, wo and ww represent the electro-osmotic permeability of oil in oil phase, oil in water phase, water in oil phase and water in water phase, respectively. In another related experimental study by [26], the diagonal component of Equation (5); K_{e-oo} and the off-diagonal component K_{e-wo} , are negligible because of the non-polarity of the hydrocarbon. Although the direct application of electric field creates a significant electro-osmotic force in the water phase, the electro-osmotic permeability of water in the water phase, K_{e-ww} has negligible impact on the condensate production. The dimension of electro-osmotic permeability of interest in this analysis is the oil in water phase, because the primary aim is condensate displacement.

Integrating results from the experimental analyses of [4], into Equation (4) and adapting Equation (5), the combined flowrate from the EK-EOR process is given in Equation (6).

$$q_{ot} = \frac{A}{\mu} \cdot \frac{1}{L} (K \cdot \Delta p + K_{e-ow} \cdot \nabla E). \quad (6)$$

From Al Shalabi et al. [27] the electro-osmotic permeability is inversely proportional to the normal permeability (Equation 7). Assuming all other factors affecting electrokinetic flow are kept constant, then

$$K_{e-ow} \propto \frac{1}{K} \quad \equiv \quad K_{e-ow} = \frac{c}{K}, \quad (7)$$

where c is a constant extracted from experimental analysis.

Replacing K_{e-ow} with expression in Equation (7) yields:

$$q_{ot} = \frac{A}{\mu} \cdot \frac{1}{L} \left(K \cdot \Delta p + \frac{c}{K} \cdot \nabla E \right). \quad (8)$$

3 | Methodology

The impact of both EKEOR and LSW process on the production performance of any reservoir can be evaluated using a full-field compositional reservoir model. Reservoir models are physics-based representations that capture the behavior of fluids within porous media under varying pressure, temperature, and compositional conditions. Reservoir simulation facilitates understanding of fluid flow behavior in the reservoir and predicts the liquid dropout ratio under varying production conditions. In this study a 3D reservoir grid model was adapted from an initial model based off on Kenyon [28] (Figure 2). The reservoir model uses a cartesian styled framework with nine cells in the x -direction, nine cells in the y -direction and four layers in the i -direction and was built using CMG GEM—a commercially available compositional simulator. Kenyon's model was originally designed for gas cycling, but for this study the injection parameters were modified to reflect water injection. The reservoir properties and PVT validation are presented in [29]. The reservoir is composed of four layers with differing permeabilities; Layer 1–130 md, Layer 2–40 md, Layer 3–20 md and Layer 4–150 md. The high permeability in Layer 4 promotes rapid movement of injected water. The injected water mixes with the aquifer water to support reservoir pressure.

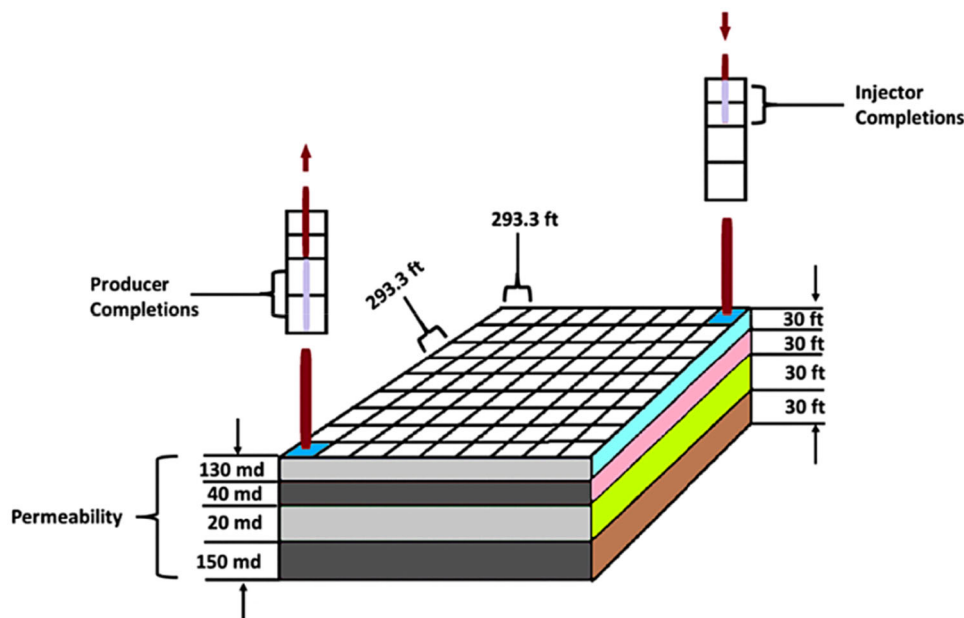


FIGURE 2 | Reservoir grid model based on Kenyon [28].

Vertical heterogeneity is defined by the four horizontal layers whose permeabilities range from 2 to 15 mD. From the data, the initial reservoir pressure is 3550 psi, temperature of 200 °F, and the rock compressibility of 3.60×10^{-6} 1/psi. Two wells were completed in the model in positions shown in Figure 2 and production simulated for 15 years. To simulate the effect of LSW and EK-EOR on gas condensate productivity, the reservoir grid data is combined with the experimental PVT data from Ikpeka et al. [4] in a compositional simulator (CMG-GEM). The compositional simulator was then validated against published laboratory data to ensure consistency in results. A detailed flowchart of the methodology adopted for this analysis is shown in Figure 3.

The relative permeability curves for the reservoir were generated using Corey's model which assumes the wetting and non-wetting phase relative permeabilities to be independent of the saturations of the other phases and requires only a single suite of gas/oil relative permeability data. Figure 4 summarizes the relative-permeability curves used in this study.

Although some minor disparities were observed at the lowest pressures shown, the plot shows an overall excellent agreement between the reservoir model and PVT data given by [28]. The pressure/volume data shows a good agreement between the reservoir model and the published data in the constant composition expansion experiment as shown in Figure 5a. This agreement is more so important within the pressure range of 2500 and 3400 psi where most of the study takes place. The biggest differences between the reservoir model and the PVT data occur around 2500 psi pressure where the highest liquid dropout varies between about 18% and 22% of the initial gas volume as seen in Figure 5b. The reservoir model forecasts a higher liquid saturation near the wellbore, and this is attributed to flow and subsequent deposition of heavier components in this area because of pressure-drop.

4 | Results and Discussions

4.1 | Condensate Flow Behavior Under Natural Depletion

The natural depletion case was first examined to establish a baseline for reservoir performance. Under natural depletion scenario, the gas rate, condensate saturation, and reservoir pressure profile were analyzed to understand the flow behavior of the condensate and the effect of condensate banking on this reservoir. During natural depletion, the production profile is driven only by reservoir pressure, with no external pressure input. To simulate natural depletion scenario, the injector for the reservoir model was shut-in during the entire production period. Both field wise analysis and localized near-wellbore production performance analysis were then conducted to understand the extent of the damage caused by in-situ retrograde condensation around the production well. The result for decline pressure in pressure against time is shown in Figure 6. As observed, a sharp decline in reservoir pressure began from the first day of production from a pressure of 3540 psi to about 3000 psi within the first year of production (322 days). This decline results in the condensation of heavier hydrocarbon components from the gas phase to the liquid phase.

This condensate dropout leads to a reduction in the effective gas saturation and affects the flow behavior of the reservoir as observed in Figure 7. The pressure decline stabilized at about 365 days and continued in a uniform decline from 2965 psi to about 550 psi after 3285 days. The pressure decline profile is indicative of a reservoir with no strong aquifer support to maintain its pressure. The gas production profile also reported increasing rates (corresponding to the decline in well pressure) within the period (0-3285 days), after which a decline in production rate was observed. The decline in gas productivity is attributable to the reduction in permeability and possible build-

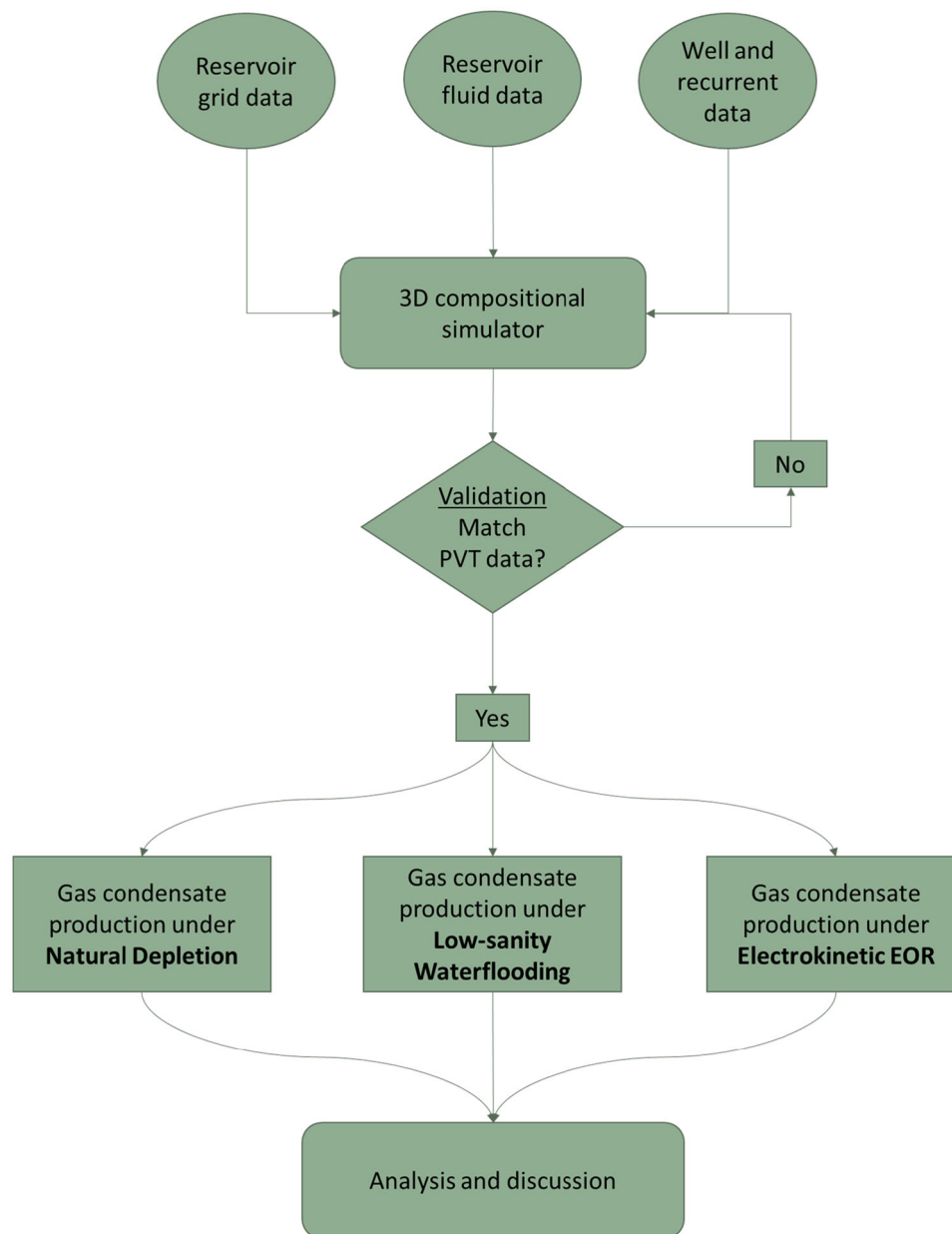


FIGURE 3 | Methodology adopted for simulating the effect of LSW and EK-EOR on condensate reservoirs.

up of immobile condensate. This gas production profile reported in this study agrees with previous study by Rahimzadeh et al. [30] who emphasized a significant reduction in well productivity owing to a sharp fall in the effective permeability of the gas. Figure 7 shows the average pressure profile within the reservoir and gas production rate taken from the production well on a linear scale.

As the reservoir pressure decreases with time, an increase in condensate saturation is observed. The saturation profile can be delineated into 3 distinct regions:

Region 3: Only the gas phase exists as the pressure is still above dewpoint pressure therefore there is no condensate dropout within this region. From Figure 7, the duration of this region was 20 days. This period is relatively small because of the rapid decrease in Well pressure observed in this study, and is

expected to increase with any external pressure intervention in the reservoir [31].

Region 2: In this region, liquid condensates begin to drop-out of the gas phase as the reservoir pressure declines below dewpoint. The first condensate saturation value was observed after 65 days. This means that between 20 and 65 days the first drop of liquid condensed out of the gas phase. At this region, the condensate saturation remains immobile and continues accumulating with the pore-space until its saturation exceeds a critical point.

Region 1: In this region, the condensate saturation exceeds the critical point and becomes mobile. Condensate saturation begins to decline as it now flows into the production well. From this analysis the critical saturation was observed to be at 16.7% at 1030 days.

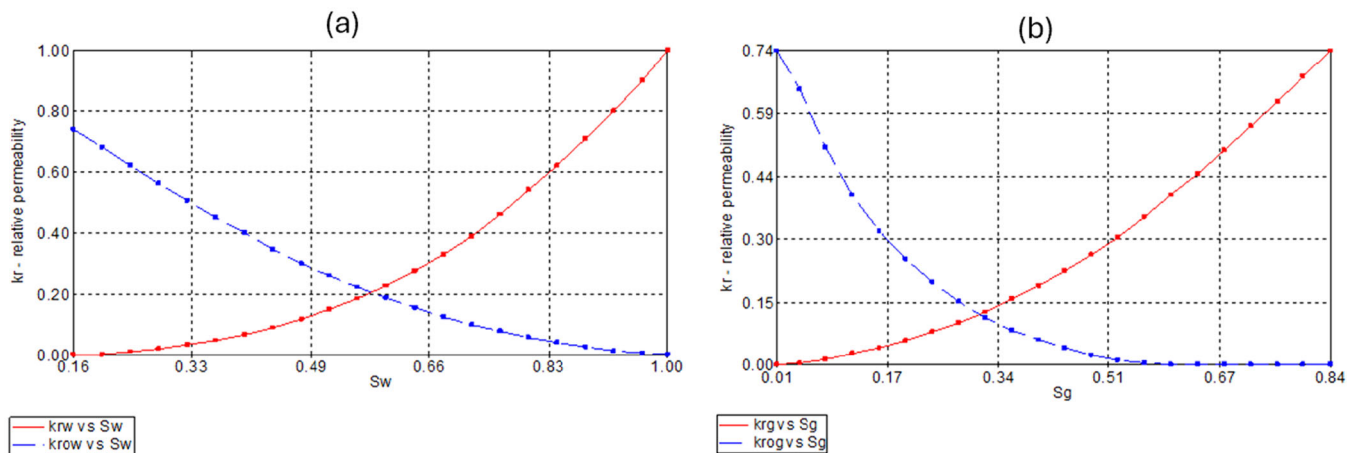


FIGURE 4 | (a) Water (K_{rw}) and Oil (K_{row}) relative-permeability curves used in simulation model, and (b) Gas (K_{rg}) and Oil [condensate] (K_{rog}) relative-permeability curves used in simulation model.

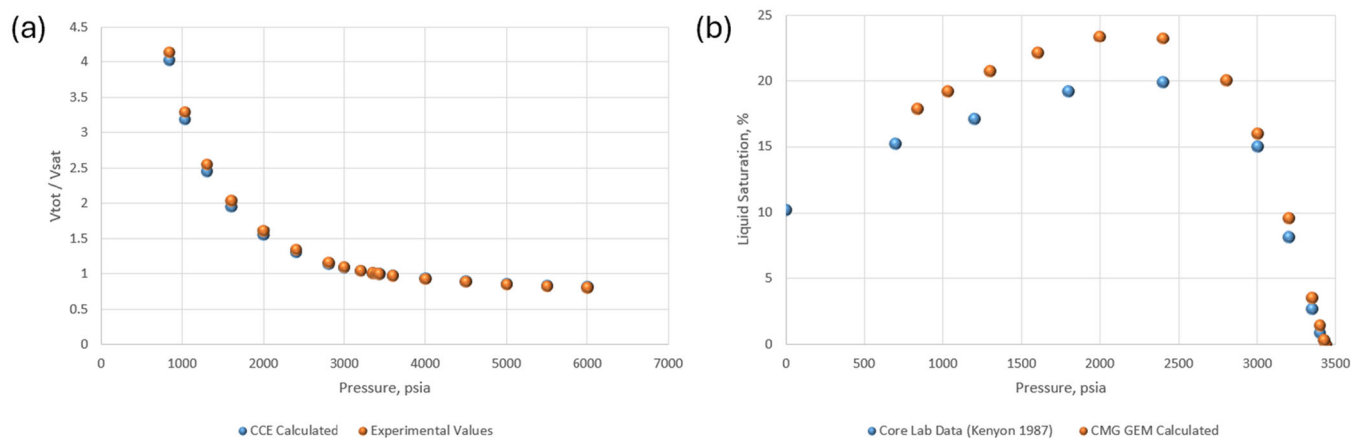


FIGURE 5 | (a) Constant composition expansion (CCE) analysis, and (b) constant volume depletion (CVD) analysis.

4.2 | Treatment of Condensate Banking With Low-Salinity Waterflooding

Low salinity water flooding is beneficial for reservoir clay stabilization, and improved water-condensate interaction due to wettability alteration [32, 33]. LSW intervention mechanism was triggered when the bottom hole pressure of the producer fell below 2500 psi. Brine was injected at 3500 psi and 3000 bbl/day for the remainder of field life. As observed in Figure 8, the initial rapid pressure decline is halted by the pressure support from the injected water. However, as the production continues at constant rate, the additional pressure support from the injected brine was not sufficient to maintain reservoir pressure and the overall reservoir pressure continues to decline. The impact of the injected brine on the gas production rate is significant—first the peak gas production rate increases from 1.78 to 1.92 mmscf/d, then an additional 520 days of more production before decline in rate is observed.

Interestingly, the average condensate deposition appeared to have been reduced by the injection of low salinity brine as shown in Figure 9. During low salinity waterflooding, the pressure of bypassed gas trapped by the water begins to decrease and condensate precipitation begins. The condensate

saturation continues to increase until it exceeds the critical point and flows into the production well. The effect of low salinity water flooding on the condensate bank is only felt after a stabilized condensate profile is attained. The explanation for this behavior can be attributed to the piston effect of the low salinity brine on the deposited condensate [34, 35].

As a result of the pressure decline in the reservoir, the composition of both the gas and condensate also changes dynamically with time. This change is reflected on the mole density profile of both the gas and condensate in Figure 10. It is noted that while a steep gradient was observed for change reservoir fluid composition (oil and gas mole density) during natural depletion, the change in composition during low salinity waterflooding was more gradual. For example, after 3250 days of production, the gas mole density decreased by 27% while the condensate mole density decreased by 82% during waterflooding compared against 30% for gas and 85% for condensate during natural depletion. The profile of the IFT between the gas and condensate showed a steady and consistent increase from the start of the production to about 3800 days. The change in IFT mirrors the pressure decline in the reservoir and increases from an initial value of 0 N/m to a maximum value of 0.012 N/m.

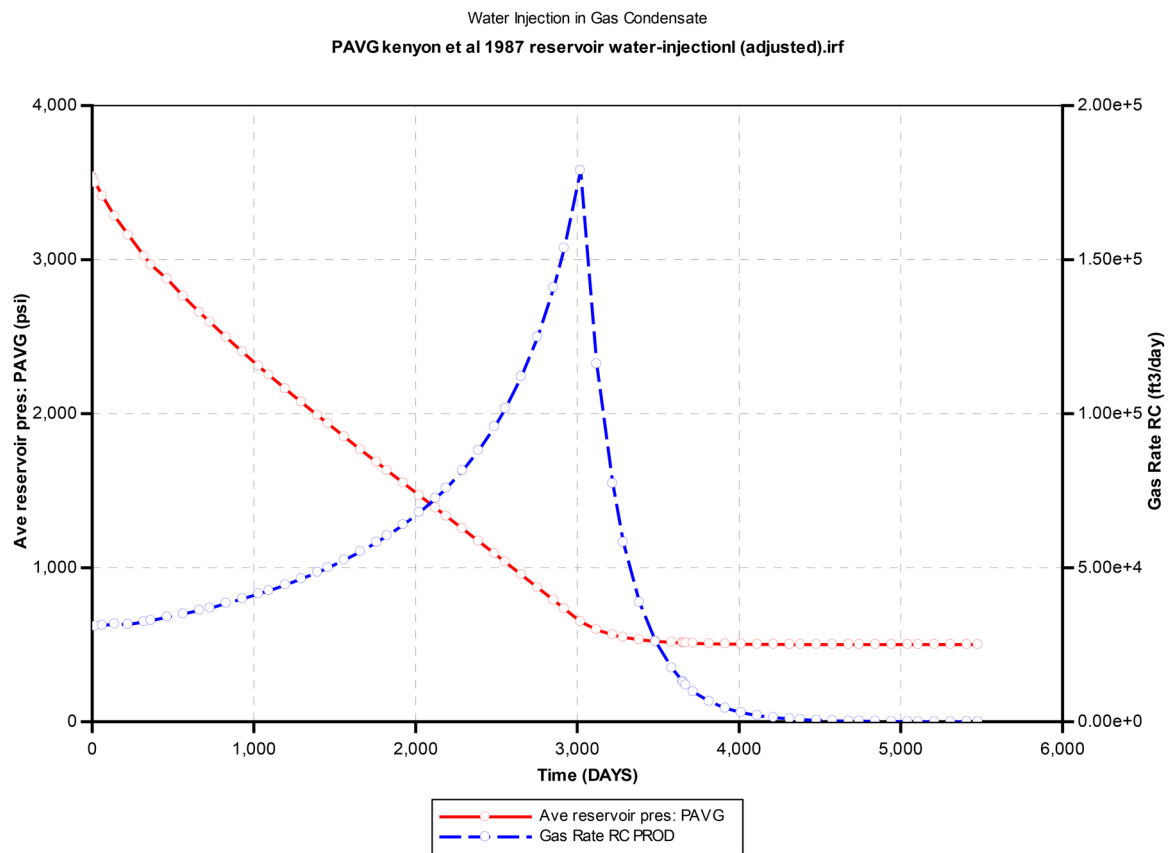


FIGURE 6 | Pressure and gas rate decline over time.

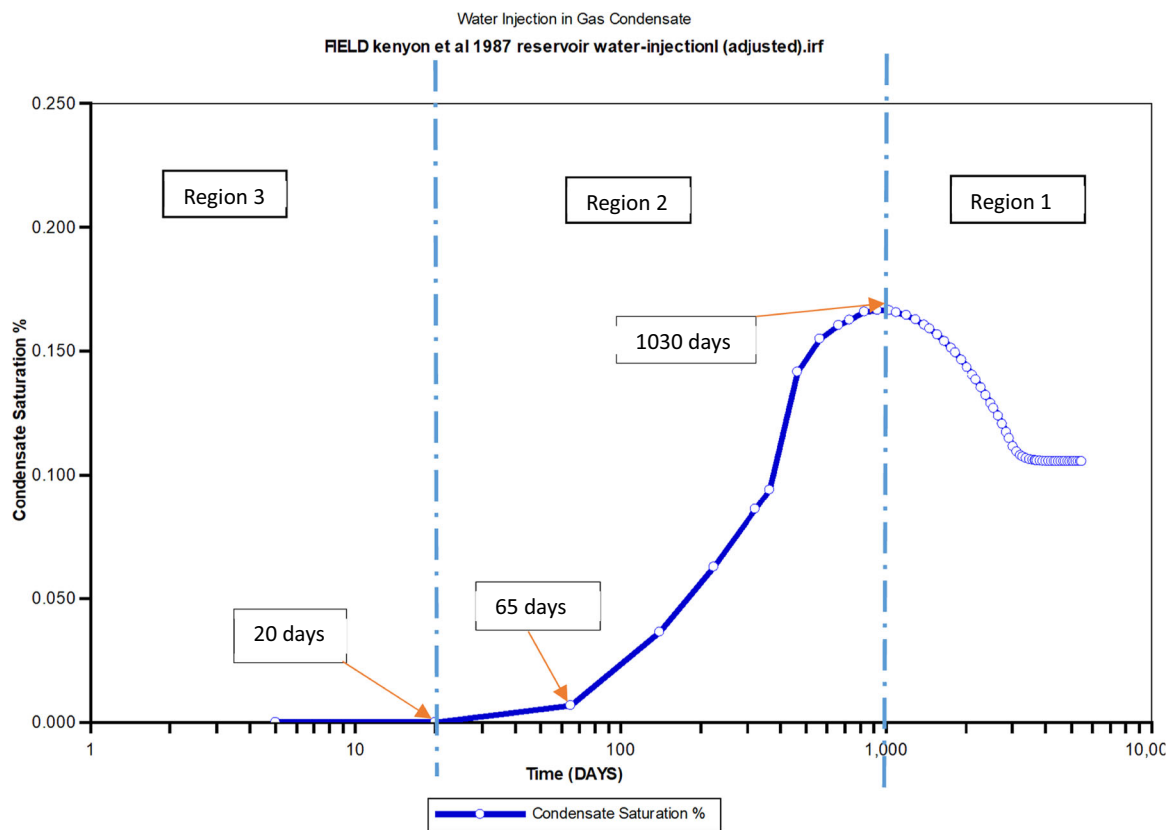


FIGURE 7 | Condensate saturation in the reservoir as a function of time.

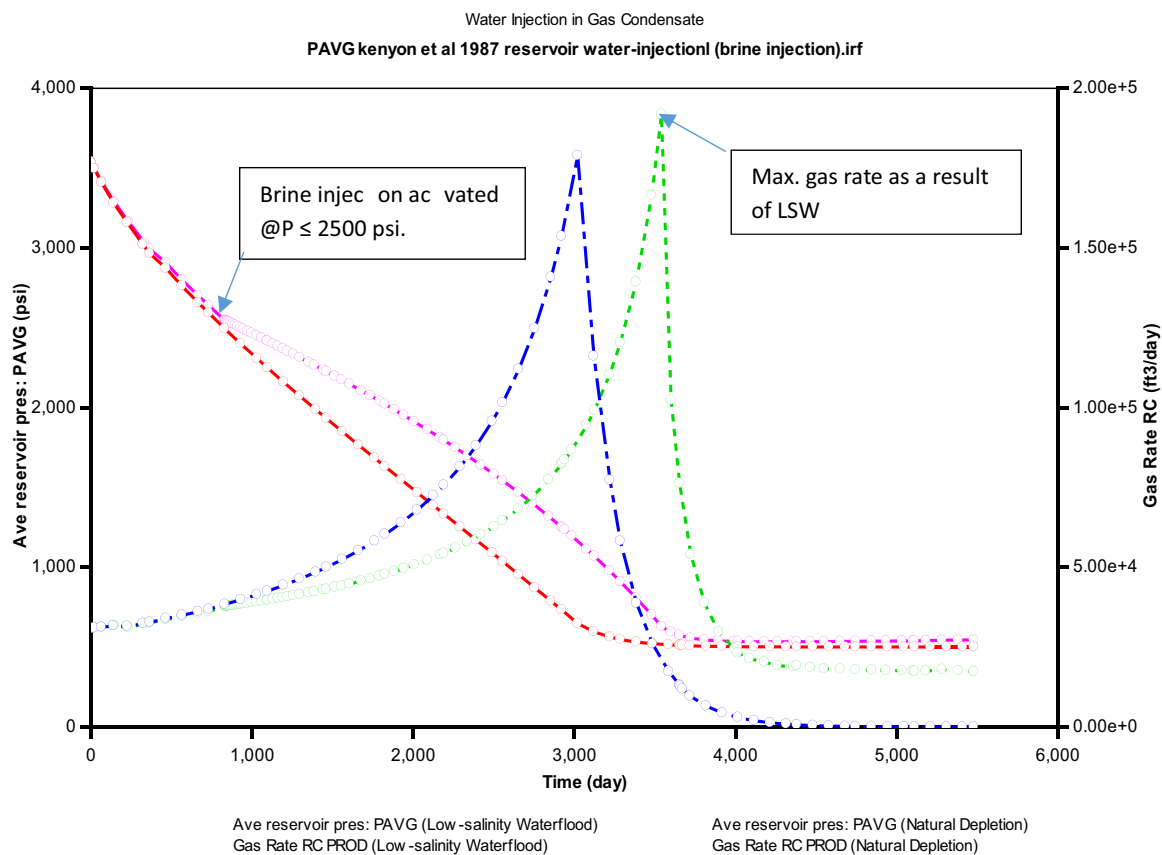


FIGURE 8 | Comparison of performance of LSW against natural depletion.

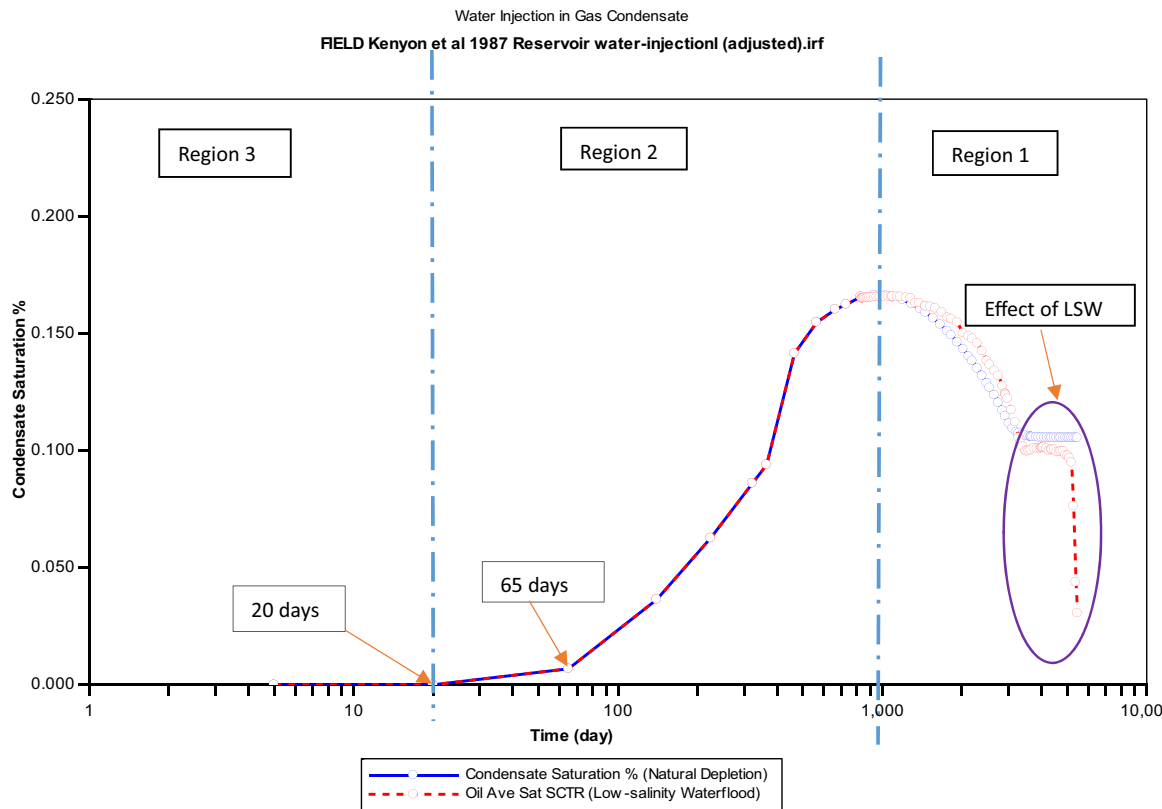


FIGURE 9 | Effect of LSW on average condensate drop-out.

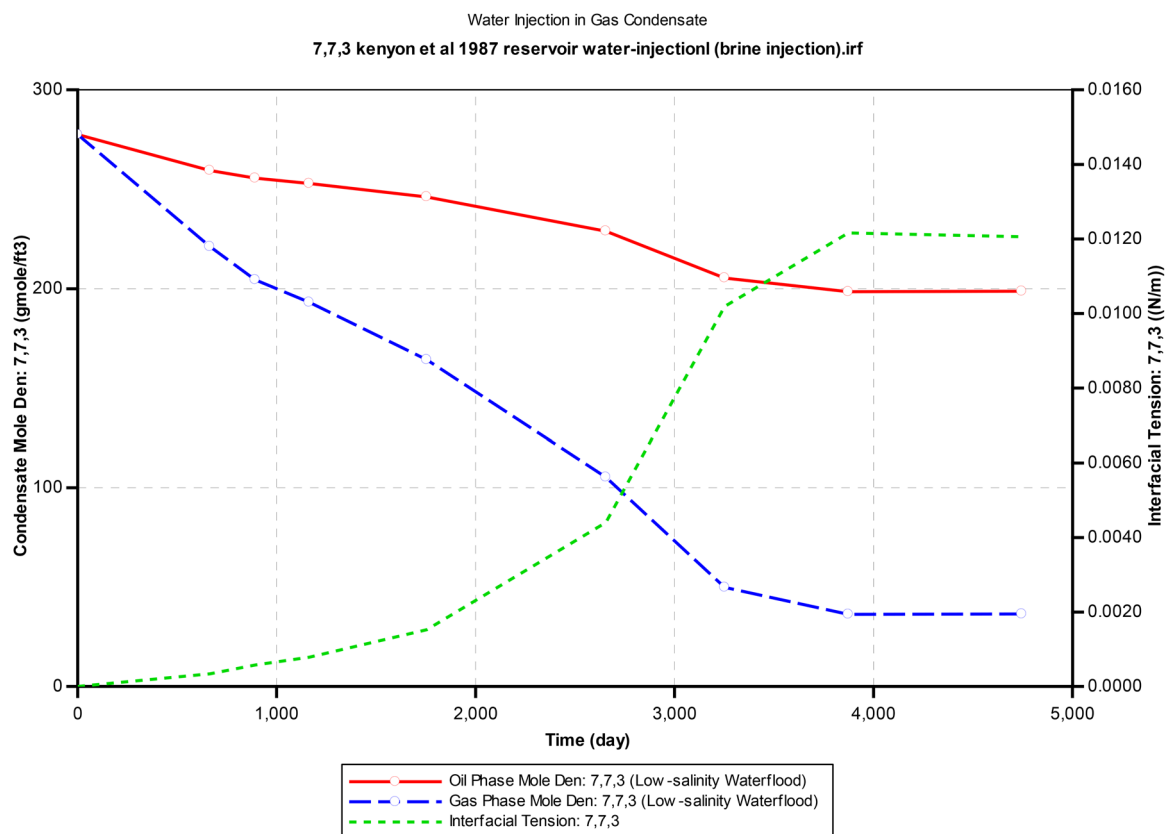


FIGURE 10 | Change in composition of gas and condensate during LSW.

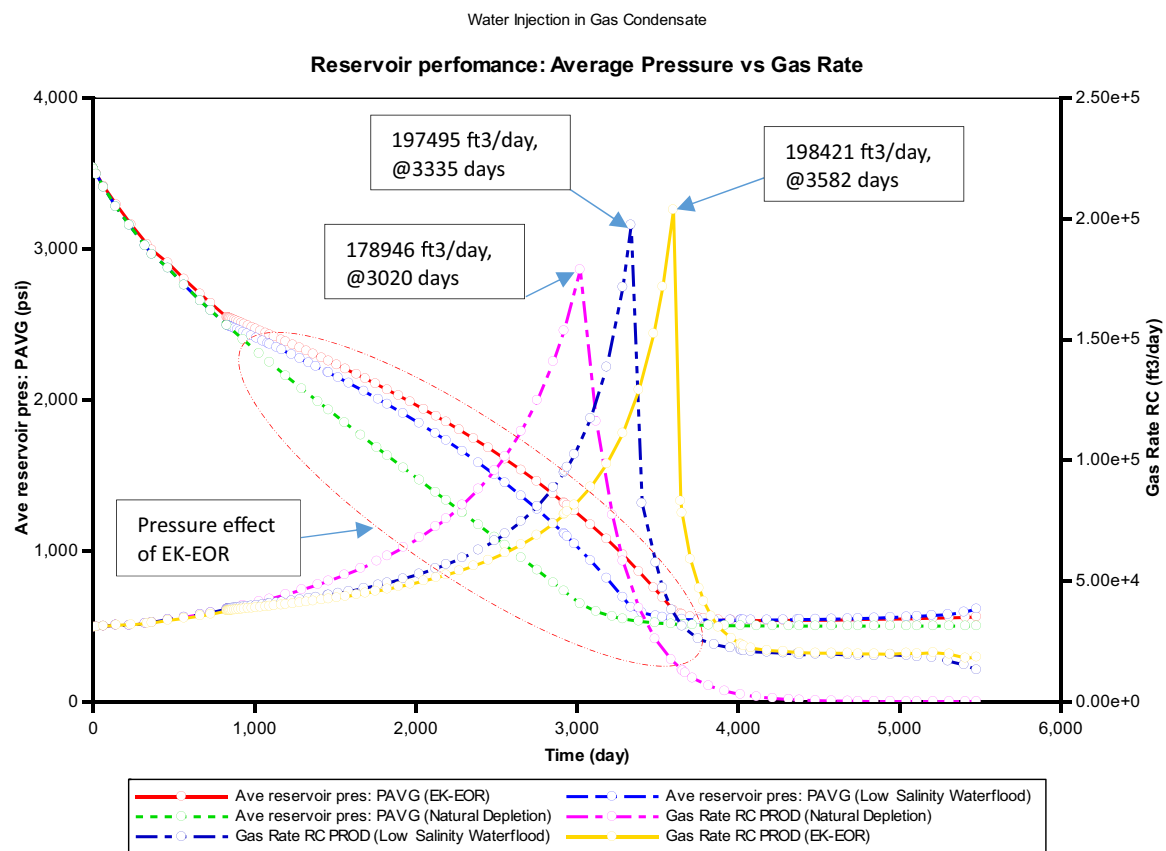


FIGURE 11 | Reservoir performance—comparing Natural Depletion, LSW against EK-EOR.

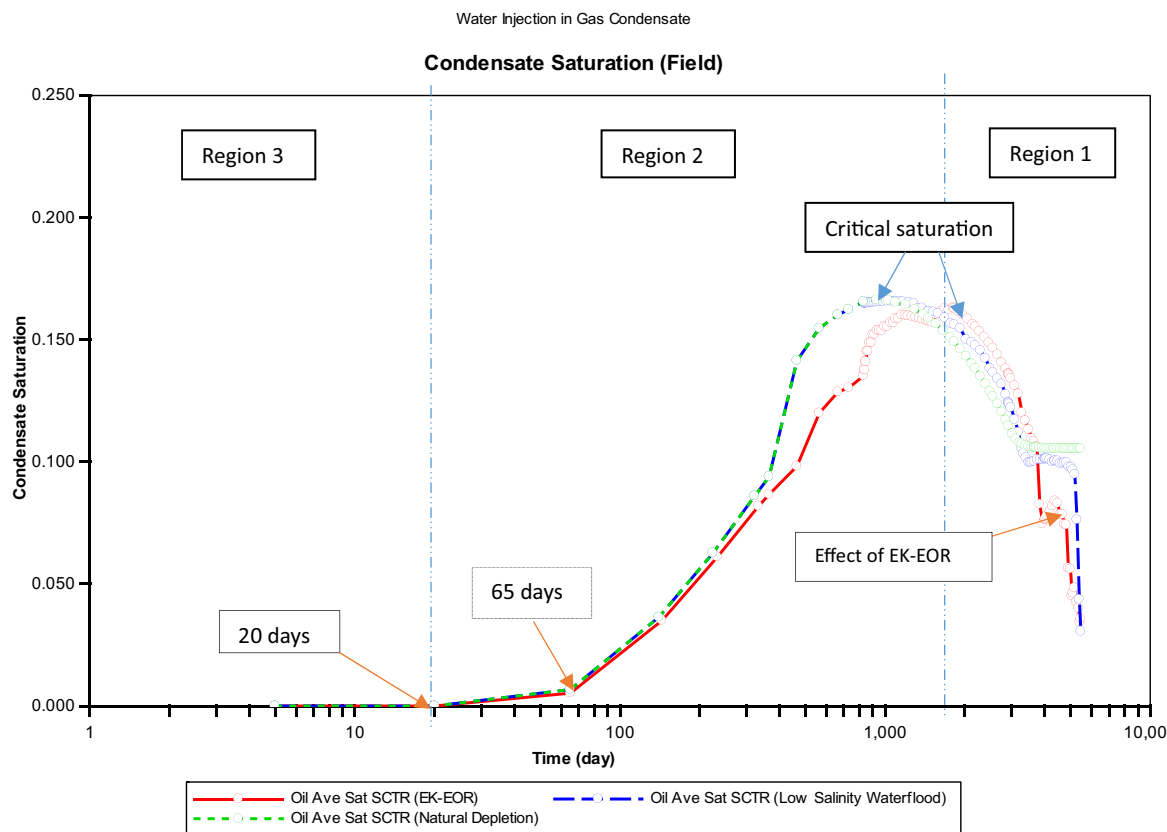


FIGURE 12 | Condensate saturation profiles during Natural depletion, Low-salinity waterflood and EK-EOR.

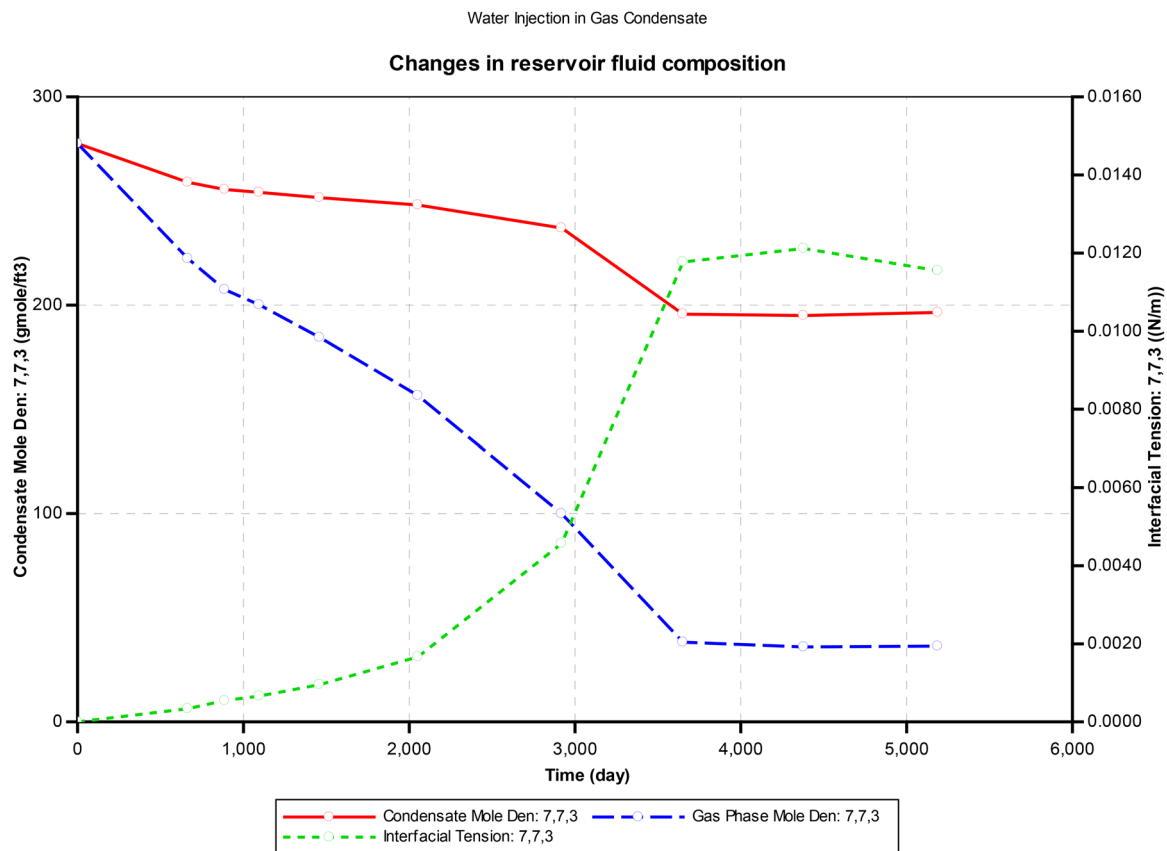


FIGURE 13 | Fluid composition changes during production.

4.3 | Treatment of Condensate Banking With EK-EOR

To simulate EK-EOR treatment in the reservoir, an electric potential is applied across the production and injection wells. The EK-EOR process builds on the low salinity waterflood treatment. Previous experiments by Yim et al. [36], confirm that EK-EOR is ineffective with a higher salinity brine because of salt precipitation at the electrodes and consequent formation damage. From the experimental analysis in [4], the effect of EK-EOR is anticipated at both the macroscopic and microscopic levels. At the macroscopic level, change in relative permeability to oil is observed while at the microscopic level, a change in the IFT is recorded. To simulate the effect of EK-EOR using CMG GEM, IFT and relative permeability curve of the water-condensate is adjusted by integrating Equation (8) into the reservoir flow equation.

An increase in IFT between the injected low salinity brine and condensate dropout causes a corresponding change in the reservoir pressure dynamics during the flooding process. When the EK-EOR effect is simulated, a significant increase in average reservoir pressure was observed in Figure 11. The effect of EK-EOR in reservoir pressure is also reflected on the gas rate. From the analysis, we observed an increased peak gas production rate higher than that obtained from the low salinity waterflood and natural depletion. The result obtained in this analysis is consistent with previous studies by Abou Sayed et al. [37]. However, one key aspect of the effect of EK-EOR is the delayed peak rate which is a consequence of changing reservoir pressure profile. In addition to the changes in reservoir pressure profile, EK-EOR also affects the condensate saturation in the reservoir as seen in Figure 12. Whereas LSW decreases the saturation through a piston-like displacement process, EK-EOR decreases the saturation by altering the deposition path.

During EK-EOR, the electroosmotic permeability to oil increases and as a result, water displaces condensate via viscous dragging. However, some areas of the reservoir are bypassed by the low salinity brine and the condensate saturation continues to build within the bypassed region because of reservoir heterogeneity. Ultimately, the condensate saturation attains a critical level beyond which it begins to flow. The path of flow for the mobile phase of the condensate differs from that of low salinity waterflood. This path is also a function of the compositional changes in gas condensate saturation during production as seen in Figure 13. It is noted that whereas a less steep gradient was observed for change in condensate and gas mole density during LSW compared to natural depletion, an even less change in composition was observed during EK-EOR process. After 3250 days of production, the gas mole density decreased by 20% while the condensate mole density decreased by 78% compared to 27% and 82%, respectively, during low salinity waterflooding. The change in IFT mirrors the pressure decline in the reservoir and increases from an initial value of 0 N/m to a maximum value of 0.0115 N/m. Whereas the final IFT is slightly lower for the EK-EOR compared to the LSW. Another profile of the IFT between the gas and condensate, for EK-EOR is like that of low salinity waterflood. A summary of the key performance index of each condensate treatment technique is provided in Table 1.

TABLE 1 | Summary of key impact of each condensate treatment technique.

Technique	Peak gas production rate	Change in condensate mole density after 3250 days	Condensate recovery	Peak condensate saturation	Time to peak gas rate	Key mechanism
Natural Depletion	1.78 mmcsf/d (baseline)	85%	Baseline	Peaks at ~38%, flows after 1030 days	3020 days	Pressure depletion only
LSW	1.92 mmcsf/d (+7.87% vs baseline)	~3% reduction vs baseline	+modest increase	Reduced by ~1.7%, flows after 1030 days	3335 days	Piston displacement, IFT reduction
EK-EOR + LSW	1.98 mmcsf/d (+11.24% versus baseline)	~8% reduction versus baseline	+228% versus baseline	Further reduced by ~5.7%, flows after 1980 days	3582 days	Electroosmotic flow + IFT reduction + wettability alteration

5 | Conclusions and Recommendations

This study was conducted using field scale numerical simulation of the EK-EOR process based on the laboratory analysis conducted in Ikpeka et al., [4]. The applied data were obtained from a published study by Kenyon [28]. Three cases of natural depletion, low salinity water flood, and combined EK-EOR and LSW were investigated. In the natural depletion study, condensate depositions commence at the start of production and quickly forms a ring of impaired regions around the wellbore. The saturation of the condensate peaks at 38%, after which it begins to flow into the production well. The compositional changes of the gas and condensate is captured by mole density changes. For the low salinity waterflood study, condensate depositions profile initially resembled that of the natural depletion study. However, the actual injection begins only after the reservoir pressure declines below 2500 psi. Piston-like displacement of deposited condensate towards the end of the production evaluation period is observed. The condensate is displaced from a stabilized 0.12% saturation to 0.03% at the end of the period under evaluation. During low salinity waterflooding, cumulative gas recovery improved by 8.87% compared to natural depletion study, whereas condensate saturation dropped by 1.7%.

When an electrical potential is introduced into the reservoir during the EK-EOR process, electroosmotic permeability of the oil in water increases. Consequently, this led to higher recovery rates due to viscous dragging of the condensate dropout during production. Analyzing the cumulative condensate and gas production at the reservoir, the EK-EOR process yielded a 4% increase in cumulative gas production while the cumulative condensate produced more than doubled with 228% when compared with the natural depletion process. This study concludes that combined EK-EOR and LSW is more effective in treating condensate banking. However, to maximize the benefits of EK-EOR, it is essential to carefully calibrate the electrical potential to achieve optimal condensate recovery. Combining EK-EOR and LSW techniques can provide a synergistic, environmentally friendly approach to condensate banking treatment. It is important to note that the results obtained from this study are limited by the model's input data, and boundary conditions. Future studies should validate these findings with core-scale or pilot field experiments under varying salinity and heterogeneity conditions.

Author Contributions

Princewill M. Ikpeka: conceptualization, data curation, formal analysis, funding acquisition, investigation, methodology, visualization, writing – original draft, writing – review and editing. **Chidiebele E. J. Uzoagba:** project administration, resources, software, validation, writing – review and editing.

Acknowledgments

The authors would like to acknowledge staff and colleagues at Protium Energy Solutions Ltd., for providing anonymized experimental and synthetic data used for this study.

Data Availability Statement

The data that support the reservoir modeling of this study are available at 10.2118/12278-PA. The experimental data on IFT were derived from

the published paper available in the public domain: 10.1007/s13202-021-01184-4.

References

1. A. Mohsin, A. S. Abd, and A. Abushaikh. Modeling Condensate Banking Mitigation by Enhanced Gas Recovery Methods (2021). <https://doi.org/10.2523/jptc-21491-ms>.
2. W. Zhang, Y. Cui, R. Jiang, J. Xu, X. Qiao, and Y. Jiang. *Journal of Natural Gas Science and Engineering Production Performance Analysis For Horizontal Wells in Gas Condensate Reservoir Using Three-region Model* 61, no. 2018 (September 2019): 226–236.
3. A. Hassan, M. Mahmoud, A. Al-Majed, et al., “Gas Condensate Treatment: A Critical Review of Materials, Methods, Field Applications, and New Solutions,” *Journal of Petroleum Science and Engineering* 177, no. 2018 (December 2019): 602–613, <https://doi.org/10.1016/j.petrol.2019.02.089>.
4. P. M. Ikpeka, J. O. Ugwu, G. G. Pillai, and P. Russell, “Effect of Direct Current on Gas Condensate Droplet Immersed in Brine Solution,” *Journal of Petroleum Exploration and Production Technology* 11 (2021): 2845–2860, <https://doi.org/10.1007/s13202-021-01184-4>.
5. N. Miller, H. Nasrabadi, and D. Zhu. Application of Horizontal Wells to Reduce Condensate Blockage in Gas Condensate Reservoirs. Society of Petroleum Engineers - International Oil and Gas Conference and Exhibition in China 2010, IOGCEC, (2010), 2(November), 1163–1177. <https://doi.org/10.2118/130996-ms>.
6. M. A. Sayed and G. A. Al-Muntasheri, “Mitigation of the Effects of Condensate Banking: A Critical Review,” *SPE Production & Operations* 31, no. 2 (2016): 85–102, <https://doi.org/10.2118/168153-pa>.
7. M. K. Alarfaj, A. Abdulraheem, and Y. R. Busaleh. Estimating Dewpoint Pressure Using Artificial Intelligence (2012). *March*, 19–21. <https://doi.org/10.2118/160919-ms>.
8. V. Bang, G. A. Pope, M. M. Sharma, J. R. Baran, and M. Ahmadi, “A New Solution to Restore Productivity of Gas Wells With Condensate and Water Blocks,” *SPE Reservoir Evaluation & Engineering* 13, no. 2 (2010): 323–331, <https://doi.org/10.2118/116711-PA>.
9. V. S. S. Bang, C. Yuan, G. A. Pope, et al. Improving Productivity of Hydraulically Fractured Gas Condensate Wells by Chemical Treatment. In Offshore Technology Conference (p. OTC-19599-MS) (2008). <https://doi.org/10.4043/19599-MS>.
10. H. A. Al-Anazi, M. A. Al-Otaibi, M. Al-Faifi, and V. V. Hilab, “Enhancement of Gas Productivity Using Alcoholic Acids: Laboratory and Field Studies,” *All Days* (2006): SPE-102383-MS, <https://doi.org/10.2118/102383-MS>.
11. M. N. Khan, F. I. Siddiqui, S. Mansur, et al. Optimization of Conventional Acid Jobs and the Historical Trend Leading to Multistage Acid Fracturing Stimulation to Increase Gas-Condensate Productivity in Carbonate Reservoirs in Saudi Arabia. In SPE Middle East Oil and Gas Show and Conference (p. SPE-141339-MS) (2010). <https://doi.org/10.2118/141339-MS>.
12. A. S. Cullick, H. S. Lu, L. G. Jones, M. F. Cohen, and J. P. Watson, “WAG May Improve Gas-Condensate Recovery,” *SPE Reservoir Engineering* 8, no. 03 (1993): 207–213, <https://doi.org/10.2118/19114-PA>.
13. L. Zuo, Y. Chen, D. Zhou, and J. Kamath, “Three-Phase Relative Permeability Modeling in the Simulation of Wag Injection,” *SPE Reservoir Evaluation & Engineering* 17, no. 3 (2014): 326–339, <https://doi.org/10.2118/166138-PA>.
14. P. Purswani and Z. T. Karpyn, “Laboratory Investigation of Chemical Mechanisms Driving Oil Recovery From Oil-Wet Carbonate Rocks,” *Fuel* 235, no. 2017 (November 2019): 406–415, <https://doi.org/10.1016/j.fuel.2018.07.078>.
15. J. V. Nicolini, H. C. Ferraz, and C. P. Borges, “Effect of Seawater Ionic Composition Modified by Nanofiltration on Enhanced Oil

- Recovery in Berea Sandstone," *Fuel* 203 (2017): 222–232, <https://doi.org/10.1016/j.fuel.2017.04.120>.
16. A. Katende and F. Sagala, "A Critical Review of Low Salinity Water Flooding: Mechanism, Laboratory and Field Application," *Journal of Molecular Liquids* 278 (2019): 627–649, <https://doi.org/10.1016/j.molliq.2019.01.037>.
 17. D. Hill, "Application of Electrokinetics for Enhanced Oil Recovery," in *Electrokinetics for Petroleum and Environmental Engineers*, eds. G. V. Chilingar and M. Haroun. John Wiley & Sons, Inc (2014), 103–155. <https://doi.org/10.1002/9781118842805.ch3>.
 18. P. M. Ikpeka, J. O. Ugwu, G. G. Pillai, and P. Russell, "Effectiveness of Electrokinetic-Enhanced Oil Recovery (EK-EOR): A Systematic Review," *Journal of Engineering and Applied Science* 69, no. 1 (2022): 60.
 19. H. Mahdiyar and M. Jamiolahmady, "Optimization of Hydraulic Fracture Geometry in Gas Condensate Reservoirs," *Fuel* 119, no. November 2016 (2014): 27–37, <https://doi.org/10.1016/j.fuel.2013.11.015>.
 20. A. Mohammad Karim and H. P. Kavehpour, "Effect of Viscous Force on Dynamic Contact Angle Measurement Using Wilhelmy Plate Method," *Colloids and Surfaces, A: Physicochemical and Engineering Aspects* 548, no. March (2018): 54–60, <https://doi.org/10.1016/j.colsurfa.2018.03.058>.
 21. R. A. Fulcher, T. Ertekin, and C. D. Stahl, "Effect of Capillary Number and Its Constituents on Two-Phase Relative Permeability Curves," *Journal of Petroleum Technology* 37, no. 2 (1985): 249–260, <https://doi.org/10.2118/12170-PA>.
 22. P. Shen, B. Zhu, X. B. Li, and Y. S. Wu, "An Experimental Study of the Influence of Interfacial Tension Onwater-Oil Two-Phase Relative Permeability," *Transport in Porous Media* 85, no. 2 (2010): 505–520, <https://doi.org/10.1007/s11242-010-9575-y>.
 23. A. A. Ansari, M. Haroun, M. M. Rahman, H. Sarma, and G. V. Chilingar, "Enhancing Depth of Penetration to Improve Capillary Number by Application of EK Low-Concentration Acid IOR in Abu Dhabi Carbonate Reservoirs," *EUROPEC 2015* (2015): 293–317, <https://doi.org/10.2118/174320-ms>.
 24. B. Ghosh, E. W. A. Shalabi, and M. Haroun, "The Effect of Dc Electrical Potential on Enhancing Sandstone Reservoir Permeability and Oil Recovery," *Petroleum Science and Technology* 30, no. 20 (2012): 2148–2159, <https://doi.org/10.1080/10916466.2010.551233>.
 25. E. W. A. Shalabi, M. Haroun, B. Ghosh, and S. Pamukcu, "The Stimulation of Sandstone Reservoirs Using DC Potential," *Petroleum Science and Technology* 30, no. 20 (2012): 2137–2147, <https://doi.org/10.1080/10916466.2010.551811>.
 26. E. Ghazanfari, S. Pamukcu, M. Pervizpour, and Z. Karpyn, "Investigation of Generalized Relative Permeability Coefficients for Electrically Assisted Oil Recovery in Oil Formations," *Transport in Porous Media* 105, no. 1 (2014): 235–253, <https://doi.org/10.1007/s11242-014-0368-6>.
 27. E. W. Al Shalabi, B. Ghosh, M. Haroun, and S. Pamukcu, "The Application of Direct Current Potential to Enhancing Waterflood Recovery Efficiency," *Petroleum Science and Technology* 30, no. 20 (2012): 2160–2168, <https://doi.org/10.1080/10916466.2010.547902>.
 28. D. Kenyon, "Third SPE Comparative Solution Project: Gas Cycling of Retrograde Condensate Reservoirs," *Journal of Petroleum Technology* 39, no. 08 (1987): 981–997, <https://doi.org/10.2118/12278-PA>.
 29. P. M. Ikpeka and J. O. Ugwu, "In Situ Hydrogen Production From Hydrocarbon Reservoirs—Modelling Study," *RSC Advances* 13, no. 18 (2023): 12100–12113, <https://doi.org/10.1039/d3ra01762a>.
 30. A. Rahimzadeh, M. Bazargan, R. Darvishi, and A. H. Mohammadi, "Condensate Blockage Study in Gas Condensate Reservoir," *Journal of Natural Gas Science and Engineering* 33 (2016): 634–643, <https://doi.org/10.1016/j.jngse.2016.05.048>.
 31. B. Bilotu Onoabaghe, P. Russell, J. Ugwu, and S. Rezaei Gomari, "Application of Phase Change Tracking Approach in Predicting Condensate Blockage in Tight, Low, and High Permeability Reservoirs," *Energies* 13, no. 24 (2020): 6551, <https://doi.org/10.3390/en13246551>.
 32. M. B. Alotaibi, R. A. Nasralla, and H. A. Nasr-El-Din, "Wettability Studies Using Low-Salinity Water in Sandstone Reservoirs," *SPE Reservoir Evaluation & Engineering* 14, no. 06 (2011): 713–725, <https://doi.org/10.2118/149942-pa>.
 33. A. N. Awolayo, H. K. Sarma, and L. X. Nghiem, "Brine-Dependent Recovery Processes in Carbonate and Sandstone Petroleum Reservoirs: Review of Laboratory-Field Studies, Interfacial Mechanisms and Modeling Attempts," *Energies* 11, no. 11 (2018): 3020, <https://doi.org/10.3390/en11113020>.
 34. E. Esmailnezhad, S. L. Van, B. H. Chon, et al., "An Experimental Study on Enhanced Oil Recovery Utilizing Nanoparticle Ferrofluid Through the Application of a Magnetic Field," *Journal of Industrial and Engineering Chemistry* 58 (2018): 319–327, <https://doi.org/10.1016/j.jiec.2017.09.044>.
 35. J. Li, S. R. McDougall, and K. S. Sorbie, "Dynamic Pore-Scale Network Model (PNM) of Water Imbibition in Porous Media," *Advances in Water Resources* 107 (2017): 191–211, <https://doi.org/10.1016/j.advwatres.2017.06.017>.
 36. Y. Yim, M. R. Haroun, M. Al Kobaisi, H. K. Sarma, J. S. Gomes, and M. M. Rahman, "Experimental Investigation of Electrokinetic Assisted Hybrid Smartwater EOR in Carbonate Reservoirs. Abu Dhabi International Petroleum Exhibition & Conference." (November 2017). <https://doi.org/10.2118/188267-MS>.
 37. N. Abou Sayed, R. Shrestha, H. K. Sarma, et al. A New Approach Optimizing Mature Waterfloods with Electrokinetics- Assisted Surfactant Flooding in Abu Dhabi Carbonate Reservoirs. SPE Kuwait International Petroleum Conference and Exhibition (2012), 1–20. <https://doi.org/10.2118/163379-MS>.